

Structural, Dimensional and Thermoelectric Properties of Melt Spun $p\text{-Bi}_{0.5}\text{Sb}_{1.5}\text{Te}_3$ A.A. Melnikov^{1,2,*}, V.G. Kostishin¹, S.A. Kichik², V.V. Alenkov²¹ National University of Science and Technology "MISIS", 4, Leninskiy Pr., 119049 Moscow, Russia² Crystal Ltd, 45B, Stantsionnaya Str., 141060 Korolev, Moscow region, Russia

(Received 19 May 2014; revised manuscript received 03 July 2014; published online 15 July 2014)

Thermoelectric melt spun $p\text{-Bi}_{0.5}\text{Sb}_{1.5}\text{Te}_3$ powders were obtained and their structural properties were studied. It was established that the crystallites constituting the powder particles are nanofragmented. Powders were compacted by vacuum hot pressing and spark plasma sintering. Thermoelectric characteristics of obtained samples were investigated in 100 K-700 K temperature range. The samples prepared by above methods possess low thermal conductivity while retaining values of the Seebeck coefficient and electrical conductivity comparable to conventional crystallized materials, thereby thermoelectric efficiency ZT reaches 1.05-1.15 at 330-350 K.

Keywords: Thermoelectricity, Melt spinning, Melt spun powders, Bismuth and antimony telluride, Spark plasma sintering.

PACS numbers: 72.15.Jf, 72.20.Pa

1. INTRODUCTION

Thermoelectricity has recently attracted an increasing interest as an alternative method of converting thermal energy into electrical energy and vice versa. Extension of applications area of thermoelectric materials is associated with increasing its dimensionless thermoelectric figure of merit ZT , equal to

$$ZT = \frac{\alpha^2 \sigma}{\kappa} T \quad (1)$$

where α – the Seebeck coefficient, V/K; σ – the electrical conductivity, $\text{Ohm}^{-1}\text{m}^{-1}$; κ – the thermal conductivity, $\text{Wm}^{-1}\text{K}^{-1}$, T – the temperature of a material, K.

Scientific researches aimed to increase the thermoelectric efficiency are associated with optimization of used materials and technologies (normal directed solidification, hot vacuum pressing, extrusion) and with a search for new materials (clathrates, skutterudites, nanomaterials) and technologies (melt spinning, spark plasma sintering).

The melt spinning is a promising technology of obtaining materials, based on ultrafast cooling of melt and mainly used for preparation of amorphous alloys in metallurgy [1, 2]. The method is in serving of melt on a rotating water cooled wheel and crystallization of a material as thin films and powders. The cooling rate can reach $10^4\text{-}10^7$ K/s [1], thereby structural properties and sizes of the crystallites should be different from a material crystallized in equilibrium conditions.

Preparation of thermoelectric materials by melt spinning technique was first described in [3, 4]. In works [5-8] materials with ZT values up to 1,5 were received. Recently, ZT values about 1,3 are confirmed by paper [9].

However, not enough attention to explanation of these results is paid. The main purposes of this work are preliminary structural analysis of the melt spun powders, test sintering by vacuum hot pressing (VHP)

and spark plasma sintering (SPS) and evaluation of properties of obtained materials.

2. DESCRIPTION OF OBJECTS AND METHODS

The melt spinning process was performed at the temperature of molten material of 650 °C. The wheel rotation speed was 1200 r/min, which resulted the crystallization rate of about $10^5\text{-}10^6$ K/s. Evaluation of surface morphology, sizes and shapes of melt spun powder particles was conducted on the scanning electron microscope (SEM) FEI Phenom. The powders were compacted by VHP at 470 °C for 20 min and by SPS at 470 °C for 5 minutes under the same applied pressures. Stabilizing annealing of compacted samples was performed at 320 °C for 12 hours in vacuum.

Radiographic examinations of melt spun powders with different particles size as well as of compacted materials were carried out using DRON-UM diffractometer, $\text{CuK}\alpha$ -radiation. The lattice parameters were determined by Rietveld method for diffraction pattern with the smallest fraction of powder (< 40 microns) owing to most averaging. The coherent scattering regions (CSR) were determined by formula:

$$d = \frac{k\lambda}{\beta \cos(\theta)} \quad (2)$$

where d – the average crystallite size, nm; λ – the wavelength of radiation used, $\lambda(\text{CuK}\alpha) = 0,154051$ nm; β – full width at half maximum, rad; θ – the diffraction angle, rad; k – the Scherrer constant = 0,9.

The measurements of the compressive strength of compacted samples were performed on the electrodynamic system ElectroPuls E1000 at room temperature.

The Seebeck coefficient (α), conductivity (σ) and the thermal conductivity (κ) of the samples with dimensions $5 \times 5 \times 10$ mm were measured before and after annealing at room temperature and after annealing in the range of 100-700 K. The lattice thermal conductivity

* kitmel@mail.ru

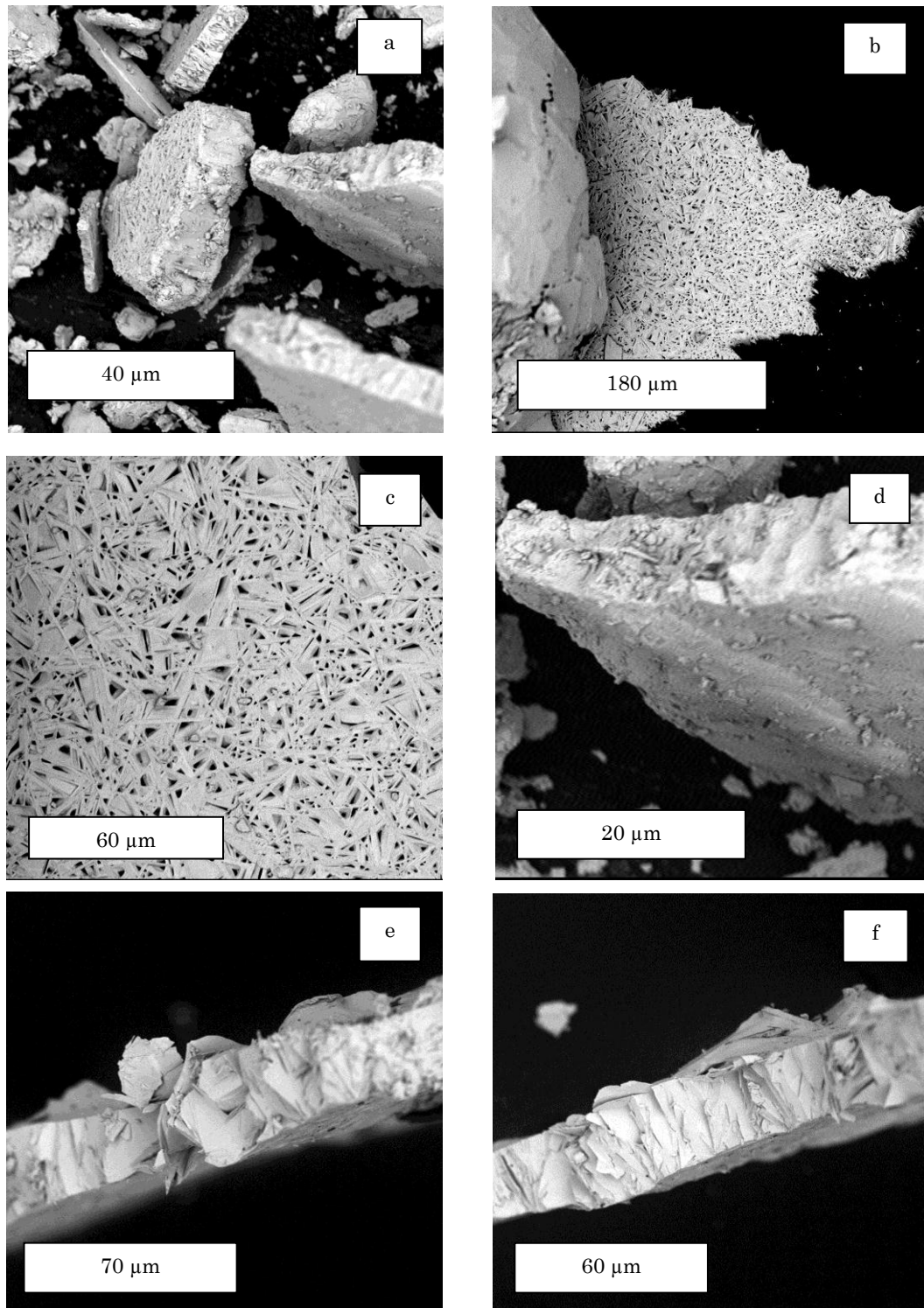


Fig. 1 – SEM images of melt spun p-Bi_{0.5}Sb_{1.5}Te₃ particles

component was determined as $\kappa_p = \kappa - \kappa_{el}$, where the electron thermal conductivity component $\kappa_{el} = A\sigma T$, where A is the Lorenz number.

Thermoelectric efficiency of materials ZT was calculated using formula (1).

3. RESULTS AND DISCUSSION

SEM images of melt spun Bi_{0.5}Sb_{1.5}Te₃ particles are shown at Fig. 1. Most of the particles have the shape of

flat plates with size ranging from tens to hundreds of microns and thickness from ones to tens of microns; the smaller particles have a bulk form (Fig. 1a).

Flat sides of particles are parallel to cooled planes of the wheel. Their surface could be completely filled with material (Fig. 1d) or with presence of gaps of crystallites (Fig. 1b, c). Such a difference in forms of surfaces of same particles is explained with peculiarity of crystallization during the melt spinning process. Af-

ter a contact with the cooled wheel the melt begin to crystallize at each point of contact, forming a continuous surface, completely filled with the material. Then, due to the high crystallization speed and the growth anisotropy in bismuth and antimony chalcogenides the material crystallizes along predominant crystallographic directions only, resulting submicron crystallites in forms of plates or polygons with gaps between them observed on the surface (1b, c).

SEM images captured in a perpendicular direction (Fig. 1e,f) give an indication of the layered structure of melt spun particles. Particle consist of plural not strictly oriented crystallites in form of flakes with thickness ranging from tens of nanometers to several microns.

X-ray diffraction patterns of powders with different size are shown in Fig. 2. Notated size is the larger linear size of a particle. The 2θ -angles of main reflection peaks of the powders patterns correspond with peaks of $\text{Bi}_{0.5}\text{Sb}_{1.5}\text{Te}_3$ crystallized under equilibrium conditions, what indicates the identity of the crystal structure; crystallographic group – $R\bar{3}m$. A slight discrepancy in the intensities of peaks with reference $\text{Bi}_{0.5}\text{Sb}_{1.5}\text{Te}_3$ is associated with partial texturing during measurements, especially for powders with larger fractions. The identity of the crystal structure suggests that the flake-crystallites formed a powder particle are the sets of alternating monolayers of atoms $-\text{Te}^{(1)}-\text{Bi,Sb}-\text{Te}^{(2)}-\text{Bi,Sb}-\text{Te}^{(1)}-$, as in crystallized under equilibrium conditions $\text{Bi}_{0.5}\text{Sb}_{1.5}\text{Te}_3$ [10]. Exfoliations along cleavage planes, probably also mainly take place between adjacent layers of atoms $\text{Te}^{(1)}$ due to lowest binding energy. Thus, we can conclude that the structure of melt spun particles differs from the structure of normally crystallized materials in orientations of crystallographic planes, surface morphology and dimensions and shapes of the crystallites.

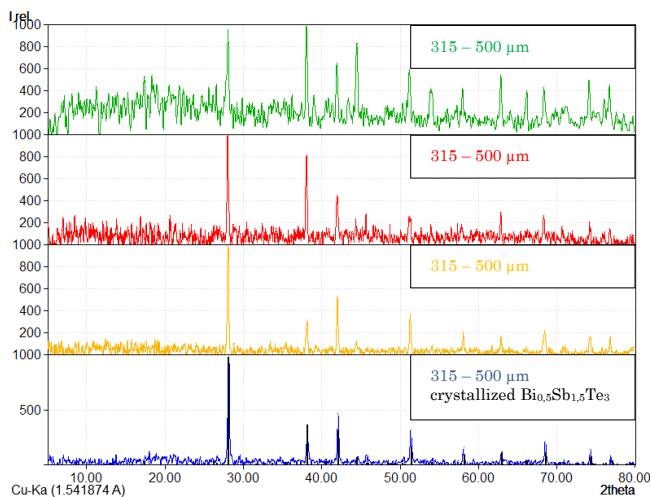


Fig. 2 – XRD patterns of melt spun $\text{p-Bi}_{0.5}\text{Sb}_{1.5}\text{Te}_3$ powders with different size

Cell parameters of melt spun $\text{Bi}_{0.5}\text{Sb}_{1.5}\text{Te}_3$ particles were determined by Rietveld method and amounted to: $a = 4,39592 \text{ \AA}$, $a = 30,51287 \text{ \AA}$.

CSD sizes of powders of different fractions are presented in Table 1. Since the sizes of CSD are estab-

lished orders of tens of nanometers, there is an evidence of nanofragmentation of crystallites, presence of defects and twinning.

Table 1 – CSD sizes of melt spun $\text{p-Bi}_{0.5}\text{Sb}_{1.5}\text{Te}_3$ particles

Particle size, μm	< 40	40-94	94-315	315-500
CSD size, nm	37,4	44,7	40,2	51,6

Melt spun powders with size of 40-94 microns were compacted by VHP and SPS. Diffraction patterns of VHP samples taken from faces perpendicular and parallel to the pressure application axis are shown in Fig. 3. An increase in intensity of [110] reflection is observed in diffraction pattern taken from the side face parallel to the pressing axis, and increase in [003] reflection is observed in pattern taken from the end face perpendicular to the pressing axis. Thus, a partial axial texture [001] directed along the pressure axis is potentially able to be formed during the melt spun powders compacting, what can be related to laying texturing and an effect of deformation processes. A more detailed studying of texture formation during melt spun powders compacting is proposed for further researches.

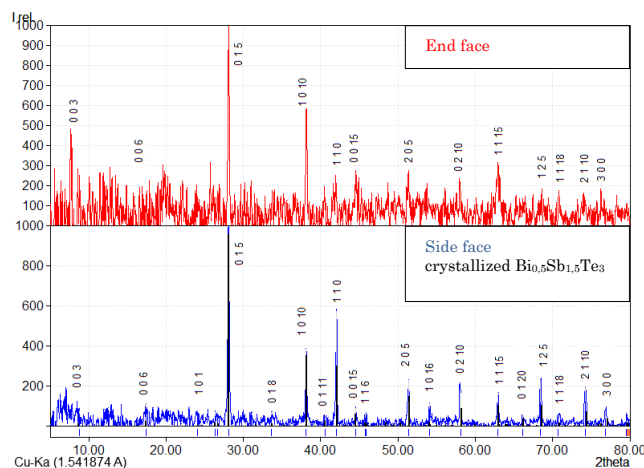


Fig. 3 – XRD patterns of melt spun $\text{p-Bi}_{0.5}\text{Sb}_{1.5}\text{Te}_3$ compacted by VHP

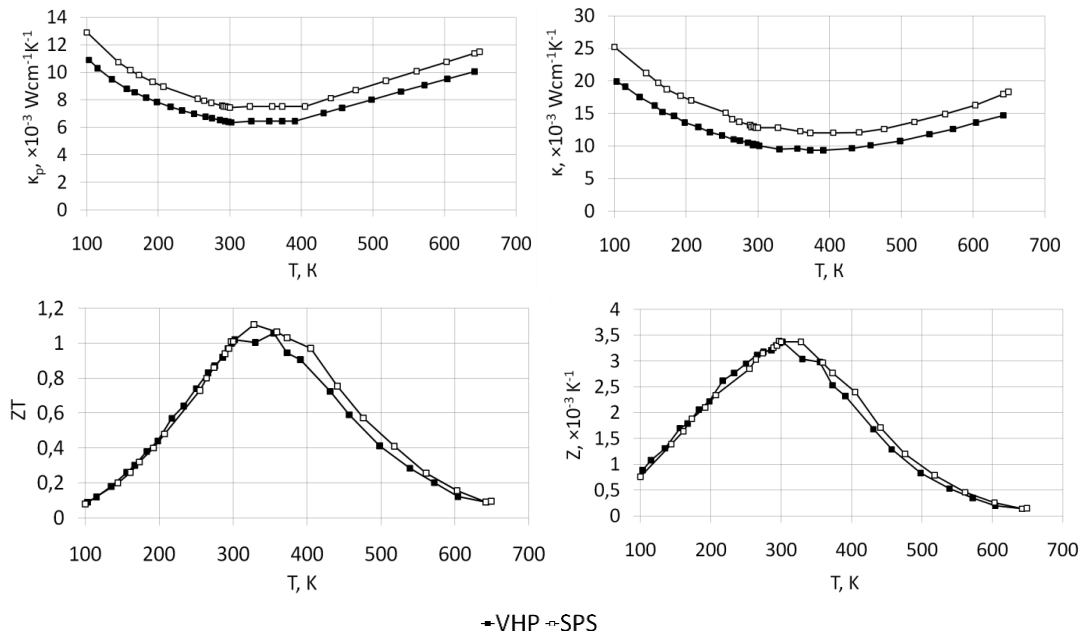
Mechanical compressive strength of compacted melt spun material amounted $65 - 75 \text{ MPa}$, which is slightly above the average compressive strength of hot-pressed mechanically divided powders – $55-60 \text{ MPa}$ [11]. These properties indicate applicability of the material for manufacturing of thermoelements and microthermoelements for Peltier modules.

Thermoelectric characteristics at 27°C of compacted melt spun powders before and after 12 hours annealing are represented in table 2. After annealing the thermoelectric efficiency Z increased for hot-pressed sample, but reduced for SPS sample, what can be explained by different structural and dimensional changes during the annealing process.

Temperature dependencies of thermoelectric characteristics of annealed samples in a direction perpendicular to the pressure axis are shown in Fig. 4. Observed values of thermal conductivity are of 10-30 % below

Table 1 – Thermoelectric characteristics of compacted melt spun $\text{Bi}_{0.5}\text{Sb}_{1.5}\text{Te}_3$ at 27 °C

	Before annealing				After 12 hours annealing			
	α , $\mu\text{V/K}$	σ , $\text{Ohm}^{-1}\text{cm}^{-1}$	$\kappa \times 10^3$, $\text{Wcm}^{-1}\text{K}^{-1}$	$Z \times 10^3$, K^{-1}	α , $\mu\text{V/K}$	σ , $\text{Ohm}^{-1}\text{cm}^{-1}$	$\kappa \times 10^3$, $\text{Wcm}^{-1}\text{K}^{-1}$	$Z \times 10^3$, K^{-1}
VHP	201	965	12,3	3,17	209	763	10,0	3,33
SPS	180	1220	11,2	3,53	198	1101	12,8	3,37

**Fig. 4** – Temperature dependences of thermoelectric characteristics of compacted melt spun $\text{p-Bi}_{0.5}\text{Sb}_{1.5}\text{Te}_3$

values of thermal conductivity are of 10-30 % below average for crystallized materials owing to a scattering of thermal phonons on grain boundaries due to structural features of the melt spun powders. The Seebeck coefficient and the conductivity values of investigated samples and crystallized materials roughly correspond. Due to this, the ZT parameter of compacted melt spun materials reach values of 1,05-1,15 in 330-350 K area.

4. SUMMARY

Structural and dimensional characteristics of $\text{p-Bi}_{0.5}\text{Sb}_{1.5}\text{Te}_3$ powders prepared by melt spinning technique are studied. The crystallographic group and the lattice parameters are identical to material crystallized in equilibrium conditions. Key features enhancing thermoelectric characteristics in melt spun powders

apparently are dimensions and shape of the crystallites, their orientation and the surface morphology.

The coherent scattering regions were defined as tens of nanometers, what suggests, that the melt spun $\text{p-Bi}_{0.5}\text{Sb}_{1.5}\text{Te}_3$ crystallites are nanofragmented.

It was found that the partial axial texture [001] directed along the axis of pressure application could be formed during the powders compacting.

Temperature dependences of thermoelectric characteristics of the material compacted by vacuum hot pressing and spark plasma sintering were measured in direction perpendicular to the pressure application axis. It is demonstrated that the compacted samples possess low thermal conductivity, thereby ZT amount reach 1,05-1,15 in 330-350 K area.

REFERENCES

1. *Physical Metallurgy* (Ed. by R.W. Cahn) (Amsterdam: Elsevier Science Publishers B.V.: 1996).
2. A.F. Belov, V.M. Glazov, Yu.V. Yatmanov, A.Ya. Potemkin, *DAN SSSR* **277**, 1155 (1984) [in Russian].
3. V.M. Glazov, Yu.V. Yatmanov, A.B. Ivanova, *Izv. AN SSSR. Neorganicheskiye materialy* **22**, 596 (1986) [in Russian].
4. O.Sh. Gogishvili, S.P. Lalykin, S.P. Krivoruchko, K.I. Puruchidi, E.S. Tsanova, *VII Vsesoyuz. konf. "Khimiya, fizika i tekhnicheskoye primeneniye khal'kogenidov*, 367 (*Uzhgorod*: 1988) [in Russian].
5. W.J. Xie, X.F. Tang, G. Chen, Q. Jin, Q.J. Zhang, *26th International Conference on Thermoelectrics*, 23 (Jeju: IEEE: 2007).
6. W. Xie, X. Tang, Y. Yan, Q. Zhang, T. Tritt, *Appl. Phys. Lett.* **94**, 102111 (2009).
7. W. Xie, X. Tang, Y. Yan, Q. Zhang, T. Tritt, *J. Appl. Phys.* **105**, 113713 (2009).
8. W. Xie, J. He, H.J. Kang, X. Tang, S. Zhu, *Nano Lett.* **10**, 3283 (2010).
9. L.D. Ivanova, L.I. Petrova, Yu.V. Granatkina, *Termoelektrichestvo* **2013** No 1, 34 (2013).
10. B.M. Gol'tsman, V.A. Kudinov, I.A. Smirnov, *Poluprovodnikovyye termoelektricheskiye materialy na osnove Bi2Te3* (Moskva: Nauka: 1972) [in Russian].
11. S.A. Kichik, A.A. Melnikov, I.S. Marakushev, A.N. Koryakin, *Termoelektriki i ikh primeneniya. Doklady XIII Mezhsosudarstvennogo seminara*, 311 (Sankt-Peterburg: FTI im. A.F. Ioffe RAN: 2013) [in Russian].